Stark Effect and Generalized Bloch-Siegert Shift in a Strongly Driven Two-Level System

Jani Tuorila,[1] Matti Silveri,[1] Mika Sillanpää,[2] Erkki Thuneberg,[1] Yuriy Makhlin,[2,3] and Pertti Hakonen[2]

[1]*Department of Physics, University of Oulu, FI-90014, Finland*
[2]*Low Temperature Laboratory, Aalto University, P.O. Box 15100, FI-00076 AALTO, Finland*
[3]*Landau Institute for Theoretical Physics, Kosygin st. 2, 119334, Moscow, Russia*
(Received 20 May 2010; published 14 December 2010)

A superconducting qubit was driven in an ultrastrong fashion by an oscillatory microwave field, which was created by coupling via the nonlinear Josephson energy. The observed Stark shifts of the "atomic" levels are so pronounced that corrections even beyond the lowest-order Bloch-Siegert shift are needed to properly explain the measurements. The quasienergies of the dressed two-level system were probed by resonant absorption via a cavity, and the results are in agreement with a calculation based on the Floquet approach.

The characteristics of matter and light become intertwined upon interaction. The interconnection of the two can be observed in atomic and optical physics by setting atoms inside mirrored cavity resonators, whereby coupling the zero-point vibrations of the field to atomic transitions. Pioneering studies of quantum physics have been carried out in the scheme (see, e.g., [1]).

Recently, an increasing emphasis has been put on the study of analogous physics in a setting of electromagnetic modes interacting with discrete systems, but in a solid-state environment. Such quantum few-level systems, or, artificial atoms, have been realized based on quantum dots and superconducting Josephson qubits [2–4].

Apart from zero-point vibrations in a cavity, natural or artificial atoms can be coupled to a driven laser field. One of the effects of the field is the dynamic (ac) Stark shift [5–9] of the energy levels. For off-resonant driving, the shift scales linearly in the number of quanta in the field. An additional correction, the Bloch-Siegert shift, appears for an oscillating, rather than circularly polarized field [10,11]. A strong drive with the Rabi frequency Ω_R becoming a sizable fraction of the atomic level spacing is needed to reveal the realm of such delicate phenomena, which poses a challenge for experimenting with real atoms. A good understanding of the physics is important also since the artificial systems hold promise for quantum information processing.

In the present work, we investigate the energy levels of an artificial two-level system driven by an oscillatory field originating from a harmonic drive via the Josephson energy. We measured large Stark shifts of the qubit level spacing unseen in atomic systems. The shifts are found to exhibit unconventional and to some extent nonmonotonic dependence on the field amplitude. This work is the first observation of a Bloch-Siegert–type of correction [12] in driven systems other than atomic systems [13] or magnetic resonance [11]. Unlike all but few previous experiments [14], we have to go beyond the usual lowest-order

such correction in order to account for the data. We refer to these additional changes in the qubit level splitting as the generalized Bloch-Siegert shift. This work differs from the previous studies on strong drive with superconducting or quantum dot qubits [5,6,15–26], where the coupling of the drive to the qubit was linear.

We use as the two-level system a single-Cooper-pair transistor (SCPT) [2,3], a superconducting qubit which consists of two small tunnel junctions with the Josephson energies E_{J1} and E_{J2}, (Fig. 1). The phase difference across the SCPT can be tuned by a magnetic flux Φ applied through a superconducting loop. In order to minimize background charge noise, the gate voltage is adjusted so that two charge states differing by one Cooper pair are degenerate [3]. Neglecting higher charge states, the
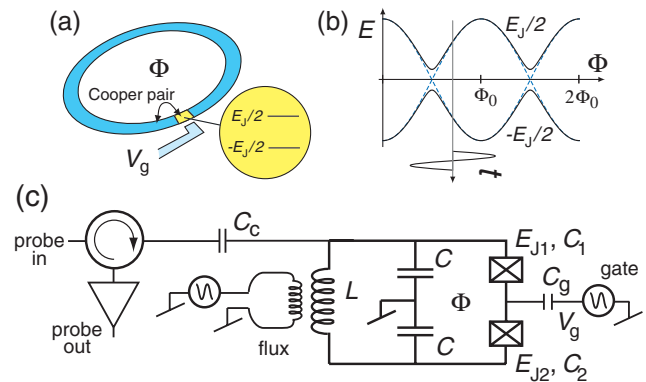

FIG. 1 (color online).   Schematic of the experimental setup. (a) The single-Cooper-pair transistor qubit consists of a superconducting loop interrupted by two Josephson junctions that separate a small island. The two relevant charge states correspond to zero or one extra Cooper pairs on the island; (b) Except near the anticrossings, the energy eigenvalues depend nearly sinusoidally on the applied flux Φ. The flux is driven likewise sinusoidally in time; (c) Detailed view of the circuit shows the microwave reflectometry readout via an LC resonator formed by on-chip lumped circuit elements [27,32].

Hamiltonian of the SCPT written in the charge basis consists of the Josephson coupling energies,

$$H_q = -\frac{E_{J0}}{2}\left[\cos\left(\frac{\pi\Phi}{\Phi_0}\right)\sigma_x - d\sin\left(\frac{\pi\Phi}{\Phi_0}\right)\sigma_y\right]. \quad (1)$$

The parameters are the total Josephson energy $E_{J0} = E_{J1} + E_{J2}$, the asymmetry $d = (E_{J1} - E_{J2})/E_{J0}$, and the flux quantum $\Phi_0 = h/2e$. The energy eigenvalues $E_J(\Phi) = E_{J0}\sqrt{\cos^2(\pi\Phi/\Phi_0) + d^2\sin^2(\pi\Phi/\Phi_0)}$ of H_q (1) are depicted in Fig. 1(b).

The applied flux $\Phi = \Phi_b + \Phi_L\cos(\omega_L t)$ consists of a static bias Φ_b and of a time-dependent microwave field with the amplitude Φ_L which is analogous to the intense laser field in atomic physics. The on-chip flux coil was designed to have a large mutual inductance of ~5 pH to the loop in order to achieve a desired fast control of the flux bias over the span of several Φ_0. Owing to the nested sinusoidal time dependence of the energy (unlike in real atoms), and unequal coupling to the different $\sigma_{x,y,z}$, the field substantially deviates from a circular polarization, and novel phenomena appear.

In the following we find the coupled states of the qubit and the field. This leads to the picture of the dressed states formed by the qubit and the microwave field. The spectrum is obtained as quasienergies, which can be considered as the characteristic energies of the combined system of the qubit and the field [1]. They repeat periodically at intervals ω_L as depicted in Fig. 2.
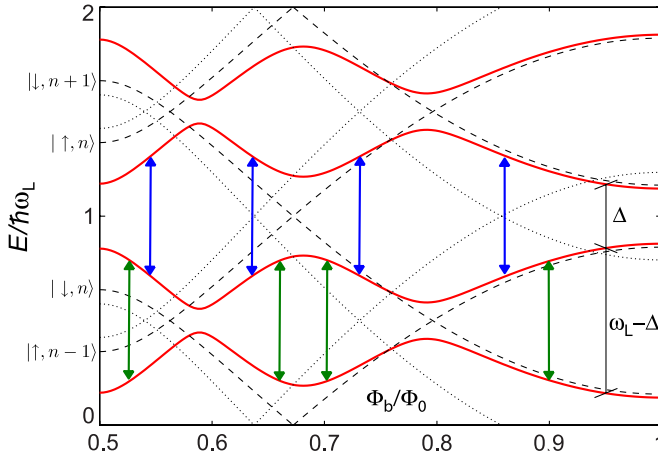

FIG. 2 (color online). Calculated quasienergies as a function of the bias flux Φ_b at $\Phi_L = 0.26\Phi_0$, and with the experimental parameters obtained by microwave spectroscopy [27]; $E_{J0}/h = 27.0$ GHz, $\omega_L/2\pi = 6.11$ GHz, and $d = 0.19$. The fully dressed states (red solid lines) are the eigenvalues of the Floquet matrix. The quasienergies repeat periodically in energy with period $\hbar\omega_L$. The level splittings are denoted by Δ and $(\omega_L - \Delta)$. The vertical green [medium gray] and blue [dark gray] arrows denote transitions induced by 3.5 GHz probe field. We also show the quasienergies of the bare states ($\Phi_L = 0$, dotted lines) and longitudinally dressed states ($\Omega_k = 0$, dashed lines).

We first diagonalize H_q (1) at $\Phi = \Phi_b$, and use these "bare" states as the basis in the following [27]. For simplicity, we give explicit formulas in the case where we keep only the 0th and 1st harmonics of the driven Hamiltonian (1). The numerical calculations, however, are done for the full Hamiltonian. To account for the temporal variation of the longitudinal field, we transform to a rotating frame. The transformation is obtained by $U = \exp[-i\sigma_z A\sin(\omega_L t)/2\omega_L]$, where $\hbar A = (2\Phi_0/\pi)J_1(\pi\Phi_L/\Phi_0)\partial E_J(\Phi_b)/\partial\Phi$. We define $\hbar\omega_0 = J_0(\pi\Phi_L/\Phi_0)E_J(\Phi_b)$, $\Omega_k = \lambda k\omega_L J_k(A/\omega_L)$ and $\lambda = 2d\sin^{-1}(2\pi\Phi_b/\Phi_0)/(d^2 - 1)$ and find

$$H_{\text{ld}} = \frac{\hbar}{2}\left[\omega_0\sigma_z + \sum_{k=-\infty}^{\infty}(\Omega_k\sigma_+ + \Omega_{-k}\sigma_-)e^{ik\omega_L t}\right]. \quad (2)$$

The strongest effect of the microwave field is a modification of the qubit splitting to $\hbar\omega_0$ by a factor of $J_0(\pi\Phi_L/\Phi_0)$. This can be understood as a rectification of the drive by the qubit nonlinearity which effectively shifts the bias point, as seen by the change from the dotted to dashed lines in Fig. 2. The positions of the resonances (level crossings), hence become shifted, cf. Fig. 2.

We consider H_{ld} (2) as a matrix operating on the longitudinally dressed states $|\sigma, n\rangle$ [15,20]. They are labeled by a qubit ("spin") index $\sigma = \uparrow, \downarrow$ and a Floquet index $n \gg 1$ indicating the number of photons in the field. Apart from that, the Ω_k terms describe transverse couplings induced by the time-dependent microwave field. The couplings shift the quasienergies from their uncoupled values (the ac Stark shift [7]). For weak couplings, $\Omega_k \ll \omega_L$, it is enough to keep only the couplings between resonant levels in the Floquet picture (rotating-wave approximation, RWA), resulting in multiphoton resonant condition $\omega_0 = k\omega_L$, where k photons are exchanged. The couplings have an effect of opening a gap at the kth anticrossing. RWA allows for analytic solutions and gives the Stark shift of $\sqrt{\delta_L^2 + \Omega_k^2} - |\delta_L|$, where δ_L is the detuning from resonance [27]. Among other approaches, RWA was sufficient for description of experiments on strongly driven superconducting qubits [15,17,20].

We fabricate our device such that the asymmetry d is significant, and Ω_k/ω_L becomes closer to 1, depending on the dc and ac bias. Hence, a few orders of the perturbative expansion in this parameter beyond RWA should be included. One of the second order contributions is the shift of the resonance frequency caused by the counterrotating term, the effect of Ω_{-1} on the $k = 1$ resonance [10]. Here, this shift is overwhelmed by other second and higher order contributions that shift the Rabi resonances (level spacing minima in Fig. 2), and constitute the generalized Bloch-Siegert shift [28].

Adding to H_{ld} (2) the photon energies, we numerically diagonalize the relevant part of the infinite Floquet matrix [28,29]. The calculated quasienergy splitting Δ for the drive amplitude $\Phi_L = 0.26\Phi_0$ is plotted in Fig. 2. Over

the full (Φ_b, Φ_L) parameter space, the splitting is shown by contours in Fig. 3(b).

In Fig. 3(b) the Rabi resonances (labeled by k) appear as light and dark tracks, corresponding to $\Delta/\omega_L \approx 1$ or 0, respectively. These resonances start as vertical lines at small Φ_L, but curve to the right with increasing Φ_L. The curving is a consequence of approaching the first zero of $J_0(\pi\Phi_L/\Phi_0)$ at $\Phi_L \approx 0.77\Phi_0$, which implies a dynamic collapse of the qubit. This effect of the nonlinear longitudinal driving bears similarity to the coherent destruction of tunneling [30] by transverse driving. It is visible as the dark horizontal band around $\Phi_L \approx 0.75\Phi_0$ in Fig. 3(b). The plot also shows several conical points (crosses), where the energy values are degenerate ($\Delta/\omega_L = 1$ or 0 exactly) [31].

Instead of measuring directly the excited state population [17], we probe the quasienergies with a weak microwave signal [27]. The probe is produced by coupling the qubit with an LC resonator via the total flux Φ in the

loop [Fig. 1(c)]. The resonator is formed by the inductance of the superconducting loop, $L \sim 410$ pH, and by the lumped element capacitors $C \sim 10$ pF made out of Al oxide between the Al films. Since the LC frequency ~ 3.5 GHz is smaller than the minimum level spacing $dE_{J0}/h \sim 5.1$ GHz of the bare qubit, the relatively weak qubit-resonator interaction does not noticeably influence the bare qubit energies.

For measurement, the LC circuit is excited at a frequency close to the resonance frequency, and the phase and amplitude of the reflected signal are recorded [27]. In the dispersive regime, where the resonator is substantially detuned from the qubit, the resonator frequency changes according to the Josephson inductance of the qubit, which was used to obtain the parameters of the qubit in the ground state. With strong drive, however, the dispersive signal becomes overwhelmed by the absorptive response. We observe an enhanced absorption (reduced reflection) of the probe field when the probe energy matches the quasienergy splitting as schematically illustrated in Fig. 2.

In Fig. 3(a), we plot the measured probe absorption obtained by driving with the microwave frequency $\omega_L/2\pi = 6.11$ GHz. Because the probe frequency $\omega_P/2\pi = 3.5$ GHz is smaller than the microwave frequency, we can see two different transitions in the absorptive measurement. These are the closest states, corresponding to energy differences $\hbar\Delta$ and $\hbar(\omega_L - \Delta)$. The resonance conditions are

$$\Delta = \omega_P \text{ (blue [dark gray]) or}$$
$$\omega_L - \omega_P \text{ (green [medium gray]),} \qquad (3)$$

where the color coding is related to Figs. 2 and 3(b). They can be interpreted as the lowest transition in a fluorescent triplet, and the transition between Rabi states [1].

In the $\Phi_b - \Phi_L$ plane, the resonance conditions appear as contours [Fig. 3(b)]. Since the matrix elements for the probe transitions are nonzero almost everywhere [27], accurate mapping of the energy landscape is possible. The resonant energy flow [32,33] from the resonator to the qubit can be seen as increased absorption as well as a phase shift in the reflection measurement. The measured locations of the absorption maxima in Fig. 3(a) follow closely the resonance lines (3) as seen by overlaying them with the theory in Fig. 3(b).

The main interest is the actual Stark shift of the spectral line, by which we mean the total energy deviation between the driven and the undriven qubit splitting, including as a part the Bloch-Siegert–type corrections. Since it is experimentally demanding to keep Φ_L fixed while changing ω_L for the spectroscopy, we fix ω_L and change the dc bias Φ_b. As seen by the qubit, the lines (3) are related to multiphoton transitions corresponding to the actual qubit splitting. We extract the Stark shift ΔE_S of the spectral line from Fig. 3 as the difference between the multiphoton energy $\hbar(m\omega_L \pm \omega_P)$ and the undriven qubit splitting $E_J(\Phi_b)$, where $\Phi_b(\Phi_L)$ parametrizes a resonance line:
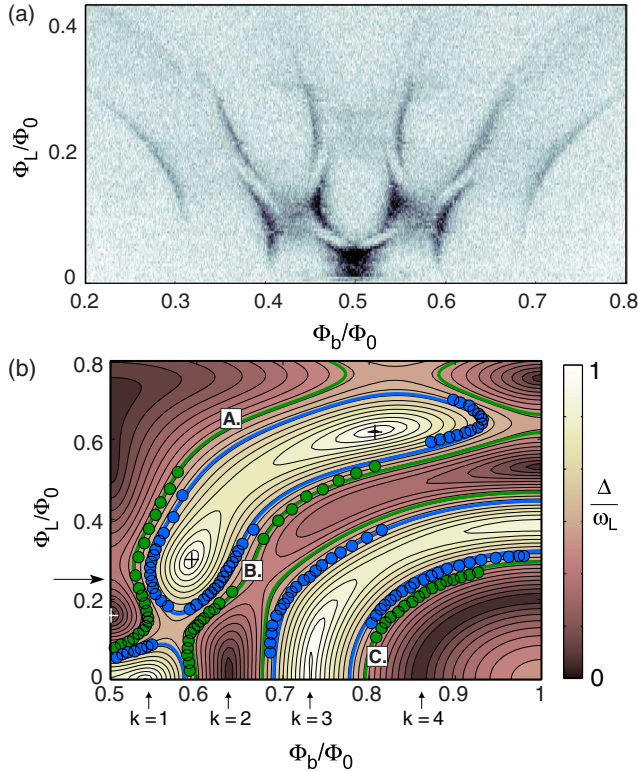

FIG. 3 (color online). (a) The measured resonance absorption of the probe signal plotted in the $\Phi_b - \Phi_L$ plane. Dark corresponds to higher absorption. The Φ_L scale is obtained by comparison to theory; (b) The landscape of the quasienergy splitting Δ calculated from the Floquet matrix of Hamiltonian (2) with the experimental parameters. The k-photon Rabi resonances appear as light (odd k) or dark (even k) tracks that are marked by index k at small Φ_L and curve to the right with increasing Φ_L. Figure 2 shows a cut along the horizontal line denoted by the black arrow. The blue [dark gray] and green [medium gray] lines denote the resonances in Eq. (3). The solid dots are the experimental resonances picked up from panel (a), or from the measured phase shift (two rightmost lines).
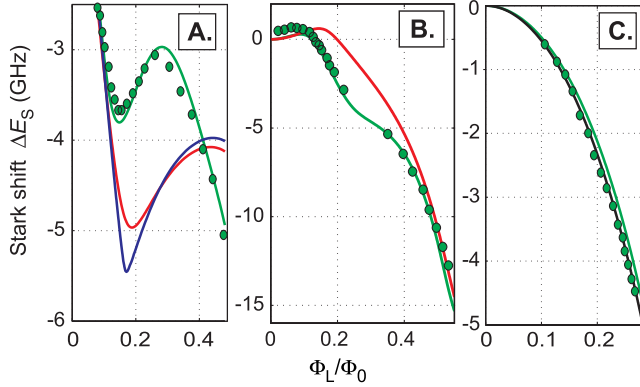
FIG. 4 (color online). The shifts of the spectral lines due to the qubit driven by a strong field. The data points for each curve A–C are picked from the resonance lines in Fig. 3 marked correspondingly. The theoretical curves were produced with the rotating-wave approximation (red [light gray] lines), or with the full numerical result (green [medium gray]). For curve A, we show also the counterrotating Bloch-Siegert correction to the RWA result (blue [dark gray]). For curve C, the black line is the analytical solution for the Stark shift, $(3\omega_L + \omega_P) \times \{1 - [J_0(\pi\Phi_L/\Phi_0)]^{-1}\}$.

$\Delta E_S(\Phi_L) = \hbar(m\omega_L \pm \omega_P) - E_J[\Phi_b(\Phi_L)]$ where the index m and the sign of ω_P depend on the spectral line and whose contour $\Phi_b(\Phi_L)$ is extracted from the measurements.

In Fig. 4 we illustrate the Stark shift of three spectral lines, marked by contours A–C in Fig. 3(b), whose multiphoton energies are $\omega_L - \omega_P$, $\omega_L + \omega_P$ and $3\omega_L + \omega_P$, respectively. The overall trend is that the shift decreases with the drive amplitude as $1 - [J_0(\pi/\Phi_L/\Phi_0)]^{-1}$ due to the rectification. Moreover, the Rabi coupling Ω_k modulates the shift near the kth resonance. Its Bessel-type dependence on the drive gives rise to the nonmonotonic Stark shift in Fig. 4. For curve C, the most relevant couplings Ω_3 and Ω_4 are small and hence the rectified level splitting ω_0 gives a good approximation, cf. Fig. 4. For curve A, resonance condition (3) is not established below $\Phi_L/\Phi_0 \lesssim 0.1$; therefore, the shift can be examined only above the threshold.

The data display a good agreement to the full theory calculations (green [medium gray]). We also show a comparison to the RWA calculation (red [light gray]), which clearly fails to explain the data. The counterrotating Bloch-Siegert correction $\Omega_k^2/(2\omega_0 + 2k\omega_L)$ provides only a small correction to the RWA result, as seen in Fig. 4, curve A (blue [dark gray]). For this resonance, higher order corrections even up to fourth order still substantially deviate from the data. The difference between the RWA prediction, and the full calculation which includes all higher orders, constitutes the generalized Bloch-Siegert shift which is verified in the measurement.

To conclude, we have investigated a superconducting qubit strongly driven via the Josephson energy. The spectral lines of the qubit experience a remarkably strong Stark shift, which necessitates us to consider higher orders beyond the rotating-wave approximation.

[1] C. Cohen-Tannoudji, J. Dupont-Roc, and G. Grynberg, *Atom-Photon Interactions: Basic Processes and Applications* (Wiley-VCH, Weinheim, 2004).
[2] Y. Nakamura, Yu. Pashkin, and J. S. Tsai, Nature (London) **398**, 786 (1999).
[3] D. Vion et al., Science **296**, 886 (2002).
[4] R. J. Schoelkopf and S. M. Girvin, Nature (London) **451**, 664 (2008).
[5] M. Baur et al., Phys. Rev. Lett. **102**, 243602 (2009).
[6] M. A. Sillanpää et al., Phys. Rev. Lett. **103**, 193601 (2009).
[7] S. H. Autler and C. H. Townes, Phys. Rev. **100**, 703 (1955).
[8] M. O. Scully and M. S. Zubairy, *Quantum Optics* (Cambridge University Press, Cambridge, England, 1997).
[9] D. I. Schuster et al., Phys. Rev. Lett. **94**, 123602 (2005).
[10] F. Bloch and A. Siegert, Phys. Rev. **57**, 522 (1940).
[11] A. Abragam, *Principles of Nuclear Magnetism* (Oxford University Press, Oxford, 1986).
[12] Bloch-Siegert shift was reported in circuit-QED by P. Forn-Díaz et al., Phys. Rev. Lett. **105**, 237001 (2010).
[13] D. Fregenal et al., Phys. Rev. A **69**, 031401(R) (2004).
[14] C. Cohen-Tannoudji, J. Dupont-Roc, and C. Fabre, J. Phys. B **6**, L218 (1973).
[15] Y. Nakamura, Yu. A. Pashkin, and J. S. Tsai, Phys. Rev. Lett. **87**, 246601 (2001).
[16] A. V. Shytov et al., Eur. Phys. J. B **36**, 263 (2003).
[17] W. D. Oliver et al., Science **310**, 1653 (2005).
[18] M. A. Sillanpää et al., Phys. Rev. Lett. **96**, 187002 (2006).
[19] K. Saito et al., Europhys. Lett. **76**, 22 (2006).
[20] C. M. Wilson et al., Phys. Rev. Lett. **98**, 257003 (2007).
[21] S. Ashhab et al., Phys. Rev. A **75**, 063414 (2007).
[22] F. Strauch et al., IEEE Trans. Appl. Supercond. **17**, 105 (2007).
[23] A. Izmalkov et al., Phys. Rev. Lett. **101**, 017003 (2008).
[24] G. Sun et al., Appl. Phys. Lett. **94**, 102502 (2009).
[25] S. N. Shevchenko, S. Ashhab, and F. Nori, Phys. Rep. **492**, 1 (2010).
[26] J. R. Petta et al., Science **327**, 669 (2010).
[27] See supplementary material at http://link.aps.org/supplemental/10.1103/PhysRevLett.105.257003.
[28] J. H. Shirley, Phys. Rev. **138**, B979 (1965).
[29] S. K. Son, S. Han, and Shih-I Chu, Phys. Rev. A **79**, 032301 (2009); J. Hausinger and M. Grifoni, *ibid.* **81**, 022117 (2010).
[30] F. Grossmann et al., Phys. Rev. Lett. **67**, 516 (1991).
[31] L. D. Landau and E. M. Lifshitz, *Quantum Mechanics* (Pergamon Press, Oxford, 1977), 3rd ed., p. 303.
[32] D. Gunnarsson et al., Phys. Rev. Lett. **101**, 256806 (2008).
[33] J. Tuorila et al., J. Phys. Conf. Ser. **150**, 022092 (2009).